Composition, Size Distribution and Characteristics of Aphron Dispersions

*Luciana Spinelli,**[1] *Amanda Bezerra,*[1] *Aline Aquino,*[1] *Elizabete Lucas,*[1] *Vitor Monteiro,*[2] *Rosana Lomba,*[2] *Ricardo Michel*[1]

Summary: This work evaluates the composition, bubble size distribution and properties of aphron dispersions. The aphrons were prepared using two types of surfactants and three different continuous phases: distillated water, brine and ester. Xanthan gum and organophilic clay were used as viscosifiers and hydroxipropilated starch as a stabilizer. The dispersions were digitally imaged under an optical microscope at 60× magnification. These images were used to determine the size distribution. Phase separation was observed in ester-based aphrons, and the phase separation progress was followed by image analysis. The percentage of incorporated air was determined by image analysis and by air compressibility. Aphrons produced from distillated water presented more bubbles and a smaller average diameter than those produced from brine or ester. Ester-based aphrons incorporated a smaller percentage of air.

Keywords: aphrons; bubbles; image analysis; microscopy; surfactants

Introduction

Aphrons, also called colloidal gas aphrons, are a dispersion of gas micro-bubbles.[1,2] Once formed, these micro-bubbles differ from the bubbles produced in air because they resist coalescence into larger bubbles and are tough and stable.[1,2] This occurs because of the micro bubbles' small size and structured walls.[2]

Aphrons are composed of two fundamental elements: a gaseous core and a thin, liquid, multi-layered protective shell, sustained by surfactants (Figure 1).[3,4]

According to Sebba,[3] besides the internal surfactant film, water-based aphrons have two additional layers that are responsible for their hydrophilic properties and mechanical resistance. Oil-based aphrons are similar to water-based ones, having an additional external bilayer.

Aphron dispersions are used in drilling fluids to minimize deep invasion into depleted high-porosity sands while stabilizing pressured shales (Figure 2).[3–8] Figure 2 illustrates the invasion process of aphrons into formation openings. At these openings the pressure is smaller than down hole, forcing the bubbles to expand, which creates a micro-environment and forms a solids-free bridge. The main properties of aphron fluids are their overall viscosity, the amount of incorporated air (related to the invasion efficiency, that is, to the volume of formation that can be occupied per volume of fluid) and the bubble size distribution (related to the internal pressure of the bubbles, that is, to the fluid energy available for expansion).

The aim of this work is to evaluate the influence of composition on the main properties of aphrons.

Experimental Setup

Three different continuous phases were used for the aphron preparations: distilled

[1] Institute of Macromolecules/Federal University of Rio de Janeiro, Centro de Tecnologia, Bl. J, Ilha do Fundão, PO Box 68525, 21945-970, Rio de Janeiro, Brazil
E-mail: spinelli@ima.ufrj.br
[2] Petrobras Research Center (CENPES), Ilha do Fundão, Q. 9, Brasil
E-mail: rlomba@petrobras.com.br

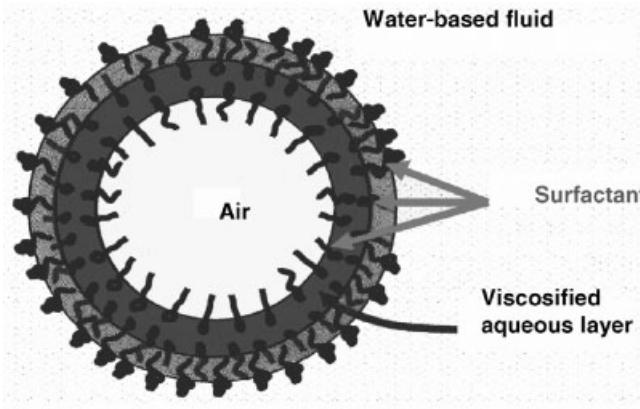

Figure 1.
Structure of a colloidal gas aphron.[3,4]

water, brine (containing 55,000 mg/L of sodium and calcium salts) and synthetic ester Liovac®3370. Two surfactants, A and B, were used as aphron generators. Surfactant A was a mixture of anionic and non-ionic surfactants and surfactant B a non-ionic polymeric fluorochemical surfactant. Xanthan gum and an organophilic clay were used as viscosifiers; a hydroxipropilated starch was used as stabilizer; magnesium oxide as pH control and glutaraldehyde as biocide. The chemicals were supplied by Petrobras (Rio de Janeiro, Brazil).

Fluids were prepared by stirring in a Hamilton Beach blender at 13000 rpm. The

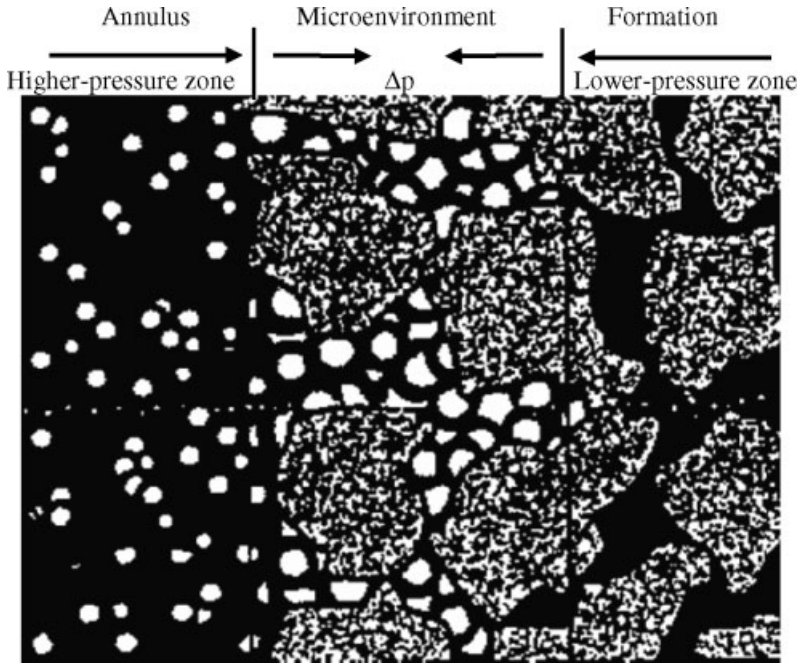

Figure 2.
Invasion process of aphrons.[3]

1 – Image aphrons.

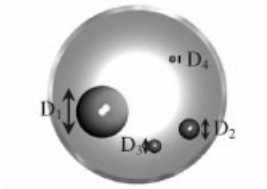

2 – Determine size distribution of bubbles.

3 – From the radius of each bubble, calculate its volume. The sum of all individual volumes corresponds to the total volume of air in that sample layer.

4 – The volume of this sample layer is defined by its area (obtained from image analysis) times the width (assumed to be equal to the diameter of the biggest bubble present in the layer.

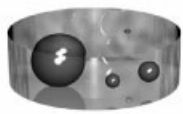

5 – The percentage of incorporated air is the ratio between the volume occupied by the bubbles and the total volume of the sample times 100%.

Figure 3.
Scheme of bubble samples on microscope slides to determine the percentage of incorporated air.

aphrons' micro-bubbles were generated in a high-pressure cell under 200 psi of pressure drop.

The micro bubble samples were imaged at different times by using a Nikon Coolpix 5400 camera attached to an Olympus SZH10 microscope at 60-x magnification. Size distributions for aphron samples were determined by image-analysis of the micro-bubbles using the AnalizeParticles routine on the Scion Image software (Scion Corp.). This software generates a list of bubble areas as a processing result. We developed a program to convert the measured areas

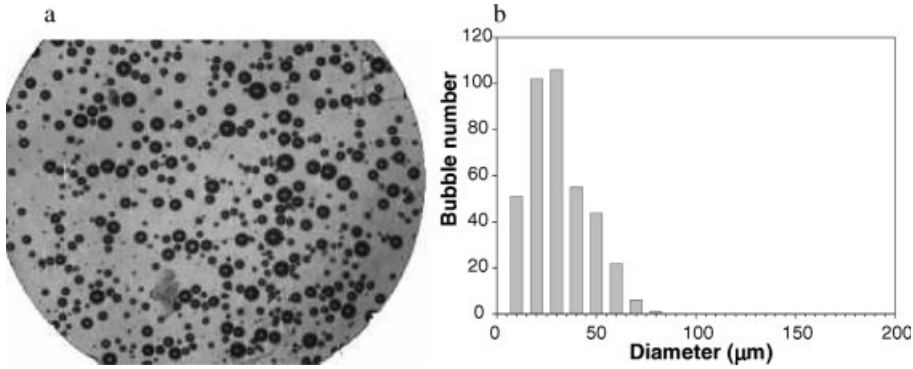

Figure 4.
Microscope image (a) and size distribution histogram (b) of AP1.

into diameter values and to group them according to size ranges. These results are presented as size distribution histograms by using plotting software.

For the samples that presented phase separation, the progress was analyzed by using the *PlotProfile* routine on Scion Image. This operation shows the intensity of light along a line drawn through the image. This line is drawn over the image in an area that contains information related to the phase separation.

The percentage of incorporated air was determined by two methods: one based on the compressibility of the incorporated air and the other on the ratio of the total image area to the area of the micro-bubbles within the image. The first method is based on compression of the aphron sample in a syringe compared with the compression of the air in the same syringe. The second method is described in Figure 3.

Results and Discussion

Water-based aphrons, prepared in distillated water and brine using surfactant A, were named AP1 and AP2, respectively. Ester-based aphrons, named AP3, were prepared in an 80:20 brine-in-ester emulsion, using surfactant B. Figures 4–6 show the microscope image (a) and the size distribution histogram (b), respectively, for samples AP1, AP2 and AP3, observed immediately after their preparation.

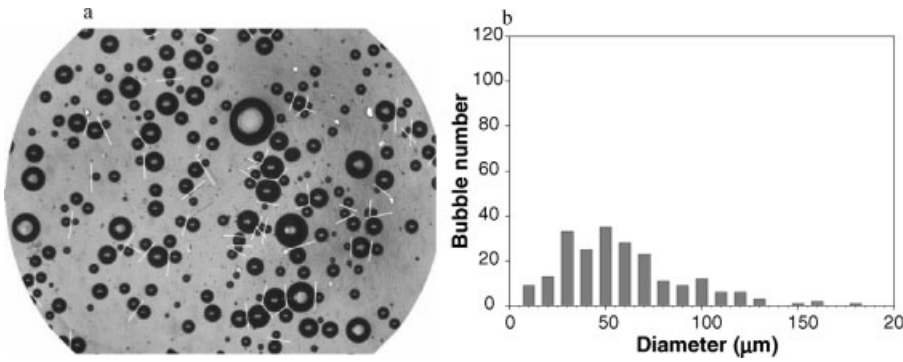

Figure 5.
Microscope image (a) and size distribution histogram (b) of AP2.

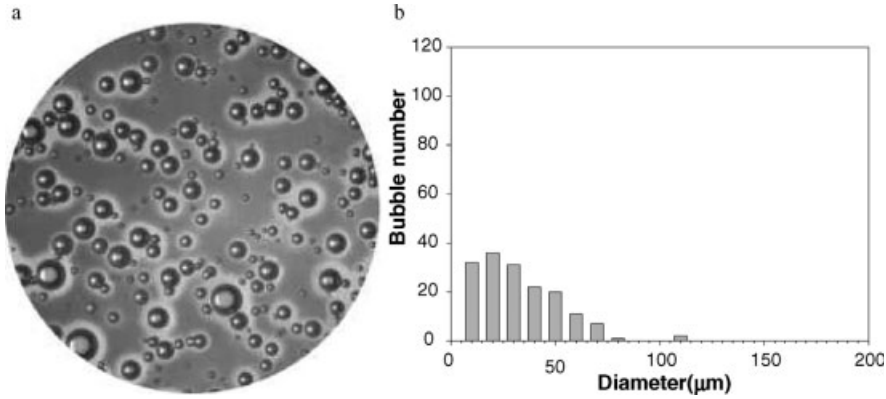

Figure 6.
Microscope image (a) and size distribution histogram (b) of AP3.

By analyzing the number of bubbles, we observed, at least at the initial time (corresponding to time = 0 s), that the number of bubbles decreased as follows: AP1 > AP2 > AP3. This observation is probably related to the stability of bubbles, which may decrease in brine and in ester when compared with distilled water.

The average bubble diameters obtained for the AP1 and AP3 samples were around 30 μm. The presence of salts (AP2) induced an increase in the average diameter (~50 μm). It is important to mention that for AP1 the size distribution of the bubbles did not change over time.

The water-based aphrons were observed to be tough and stable, as mentioned in the literature.[1,2] However, ester-based aphrons presented an evident phase separation when observed under the microscope (Figure 7).

Figure 7 shows three images obtained in sequence, 60 seconds apart. The first image was obtained as soon as the sample was collected from the aphron generator system. The phase separation is identified in these images by the appearance of the white ring around the bubble. The width of the ring increases with time. The measurement of the phase separation progress was evaluated by measuring the width of the white ring, using a plot of the light intensity *versus* position along the image, as presented in Figure 8 for the bubble's image obtained 60 s after collection of the AP3 sample.

The value used for the width of the white ring was obtained by the average of the width at half height of the two external peaks presented in Figure 8. By plotting the ring width values as a function of time, we could obtain the phase separation kinetic

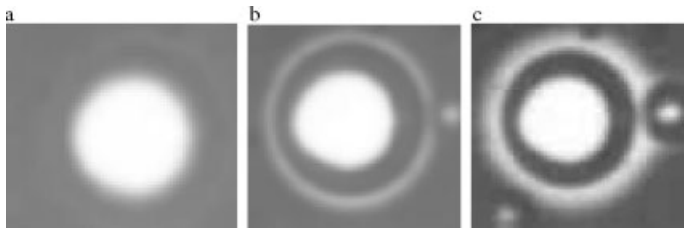

Figure 7.
Ester-based aphrons: bubble imaged at (a) 0, (b) 60 and (c) 120 s.

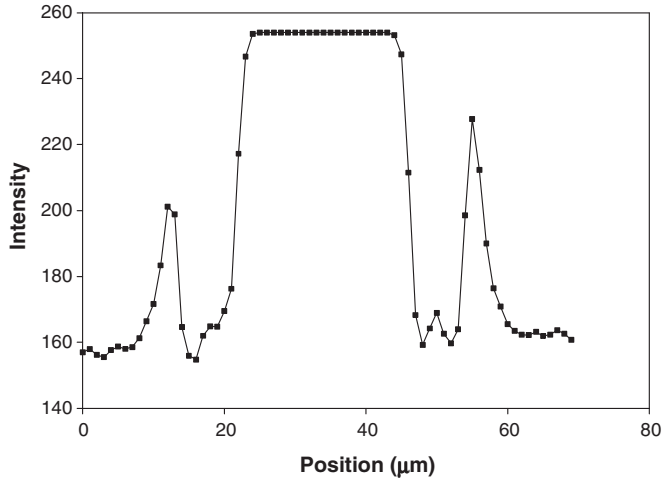

Figure 8.
Plot of light intensity *versus* position along the image for the bubble observed 60 s after AP3 sample collection.

(Figure 9) and observe, for this system, that the phase separation is more critical after 20 minutes.

The amount of incorporated air, determined by the image processing technique, was similar for water-based and ester-based aphrons, showing a value of around 15 vol%. The similarity of the results is due to the inaccuracy of this technique. It is important to note that the image processing technique produces a result that does not correspond to the total number of bubbles previously formed because the sample preparation (as a layer) destroys some bubbles in the layer boundaries.

The compressibility technique was more sensitive to the differences in the samples' air content, and was thus the preferred method for such determination. According to the compressibility technique, we observed that water-based systems prepared in distillated water or in brine presented around 22 vol% of incorporated air, while the

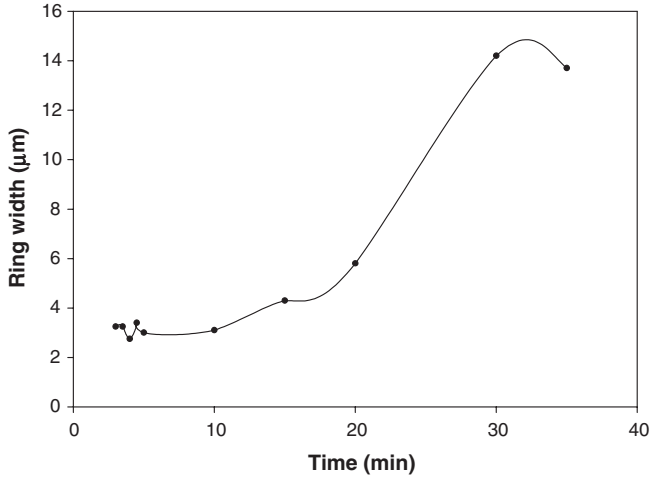

Figure 9.
Plot of ring width values *versus* time for AP3.

ester-based system incorporated around 11 vol% of air. It seems that the higher amount of incorporated air to the water-based aphrons is related to their higher stability compared with ester-based aphrons.

Conclusions

Water-based aphrons generated in distilled water showed better characteristics than ester-based aphrons because of their stability and higher amount of incorporated air. These characteristics are directly related to base-fluid composition. Also, the presence of salts contributes to an increase in the average diameter of micro-bubbles.

Phase separation in ester-based aphrons needs more study, for example, by changing the ester/water proportion. The influence of the composition on phase separation can be traced by evaluating the phase separation kinetic or by incorporated air content.

Acknowledgements: ANP/FINEP/CTPETRO, PETROBRAS, CNPq, FAPERJ, CAPES, FUJB.

[1] Y. Dai, T. Deng, *Journal of Colloid and Interface Science* 2003, *261*, 360–365.
[2] R. C. G. Oliveira, Doctoral Thesis. UFRJ, Brazil, 2004.
[3] F. B. Growcock, et al. *SPE International* 2003, 80208.
[4] C. D. Ivan, et al. *SPE International* 2002, 77445.
[5] R. Sadiq, *Sadiq Environmental Management* 2003, *32,6*, 778–787.
[6] B. D. Schaneman, et al. *American Association of Drilling Engineers* 2003, *3*, 41.
[7] Actisystem Inc. PI 9912415-7 A, April 17, 2001.
[8] Actisystem Inc. USP 6,156,708, Dec 5, 2000.

